Electronic Supplementary Material (ESI) for Sustainable Energy & Fuels.


# Supplementary Information: Organic ammonium chloride salt incorporated tin oxide electron transport layer for improving performance of perovskite solar cells

Zhigang Che, Limeng Zhang, Jiacheng Shang, Qi Wang, Yurong Zhou*, Yuqin Zhou, Fengzhen Liu*

Center of Materials Science and Opto-Electronics Engineering, College of Materials Science and Opto-Electronic Technology, University of Chinese Academy of Sciences, Beijing 100049, China

*E-mail: zhouyurong@ucas.edu.cn, liufz@ucas.ac.cn

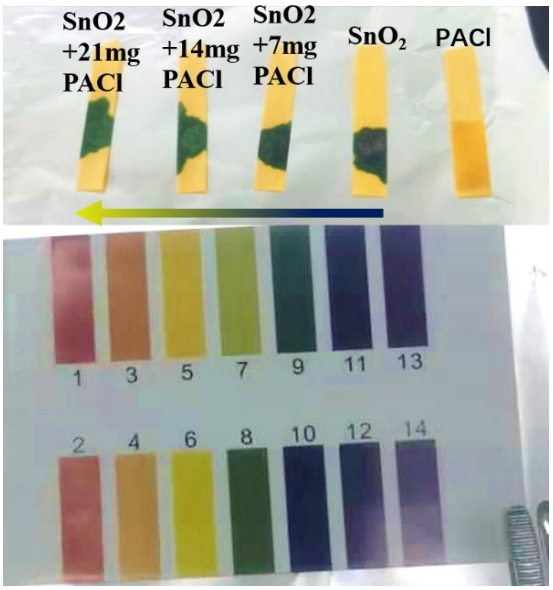


**Figure S1** PH text of $SnO_2$ colloid solution, PACl solution, and $SnO_2$ colloid solution added with PACl。

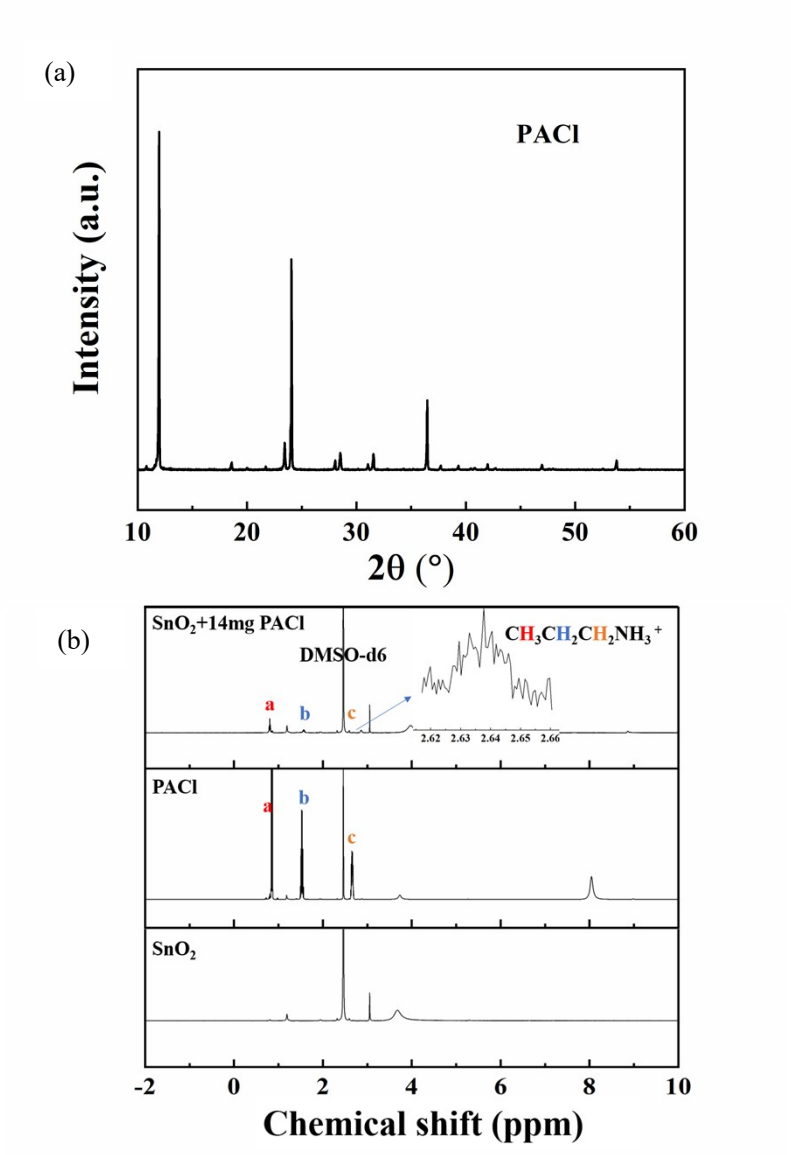


**Figure S2** (a) XRD pattern of PACl powder. (b) $^{1}$H NMR spectra of $SnO_2$ powder, PACl powder, and PACl incorporated $SnO_2$ powder, dissolved in DMSO-d6. The resonances at about 0.9, 1.5, and 2.6 ppm, marked as a, b, and c, are corresponding to -$CH_3$, -$CH_2$-, and -$CH_2$- in PA, respectively. The weak yet distinct resonance PA signals detected in the NMR spectrum of the PACl incorporated $SnO_2$ sample indicate the existence of PA in the $SnO_2$ colloid solution.

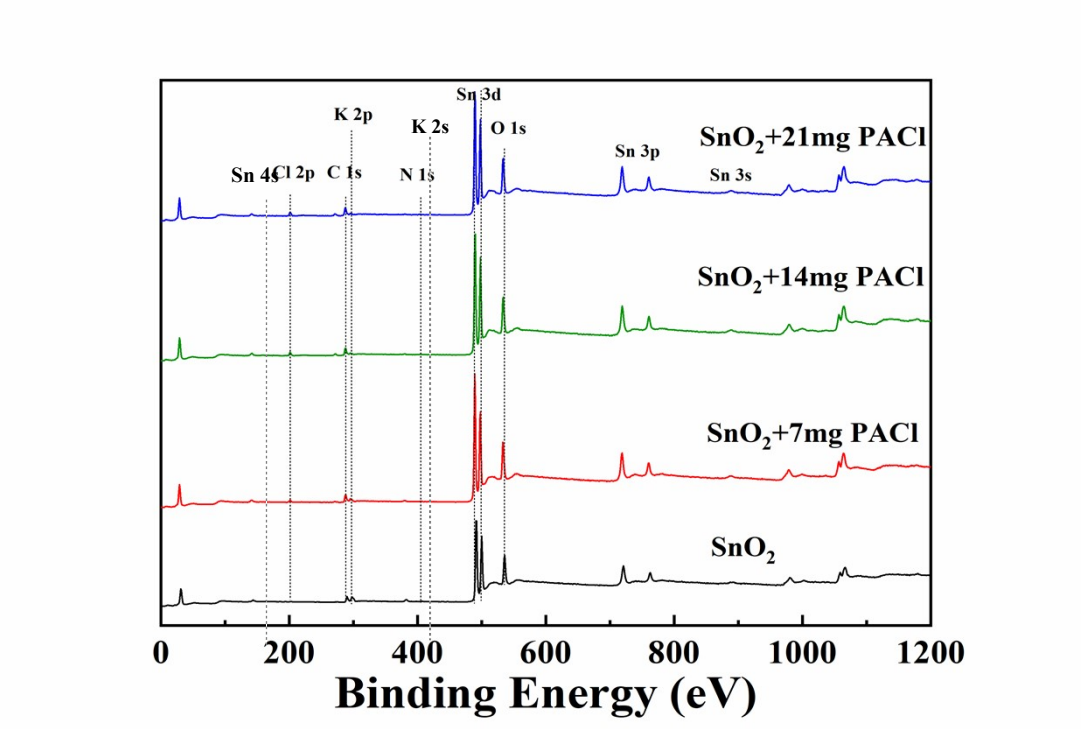


**Figure S3** XPS wide scan spectra of $SnO_2$ films with 0 mg, 7 mg, 14 mg and 21 mg PACl addition on Si substrates.

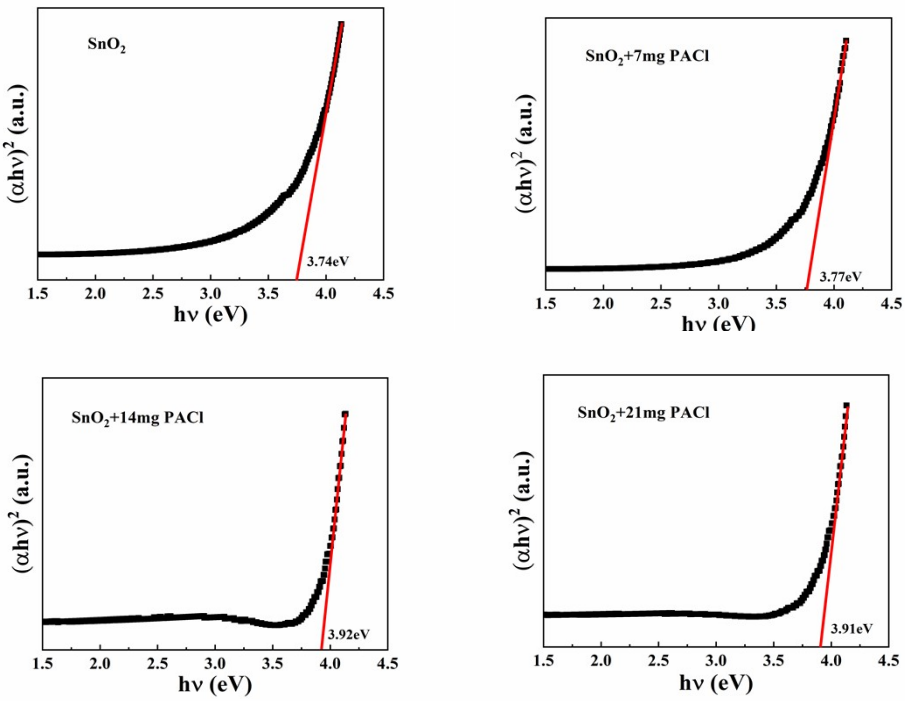


**Figure S4** Tauc plots derived from of the absorption spectra for the $SnO_2$ films with 0 mg, 7 mg, 14 mg and 21 mg PACl addition. The corresponding optical band gaps for $SnO_2$, $SnO_2$-7PACl, $SnO_2$-14PACl and $SnO_2$-21PACl films are 3.74 eV, 3.77 eV, 3.92 eV and 3.91 eV, respectively.

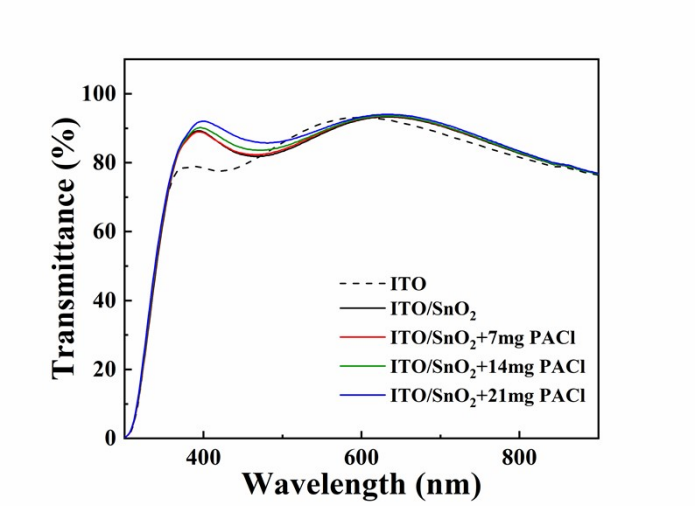


**Figure S5** Transmittance spectra of the $SnO_2$ films with 0 mg, 7 mg, 14 mg and 21 mg PACl addition. Transmittance in the wavelength range of 380-600 nm is much improved by the PACl incorporation for the $SnO_2$-14PACl and $SnO_2$-21PACl samples compared with the pristine $SnO_2$ sample. The transmittance spectrum of a ITO substrate is included.

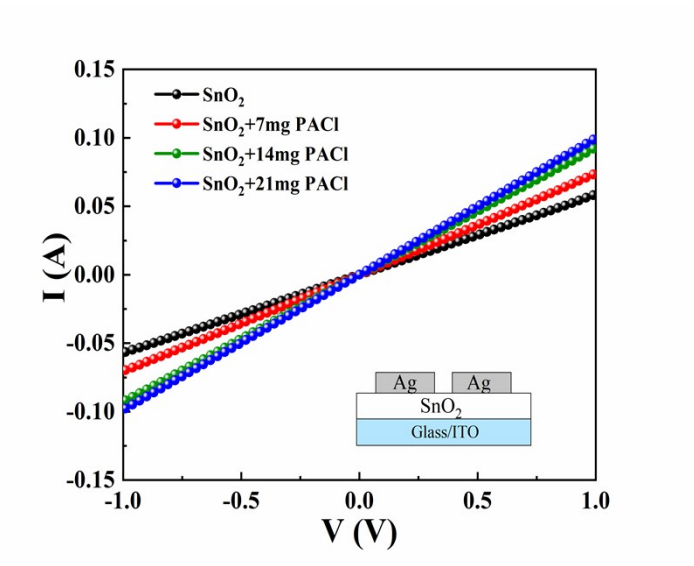


**Figure S6** I-V characteristics of simples with different ETL structures. The slope of the I-V curves increase with the increasing of the PACl concentration, which indicates improved electrical conductivity of the $SnO_2$ films by the PACl incorporation.

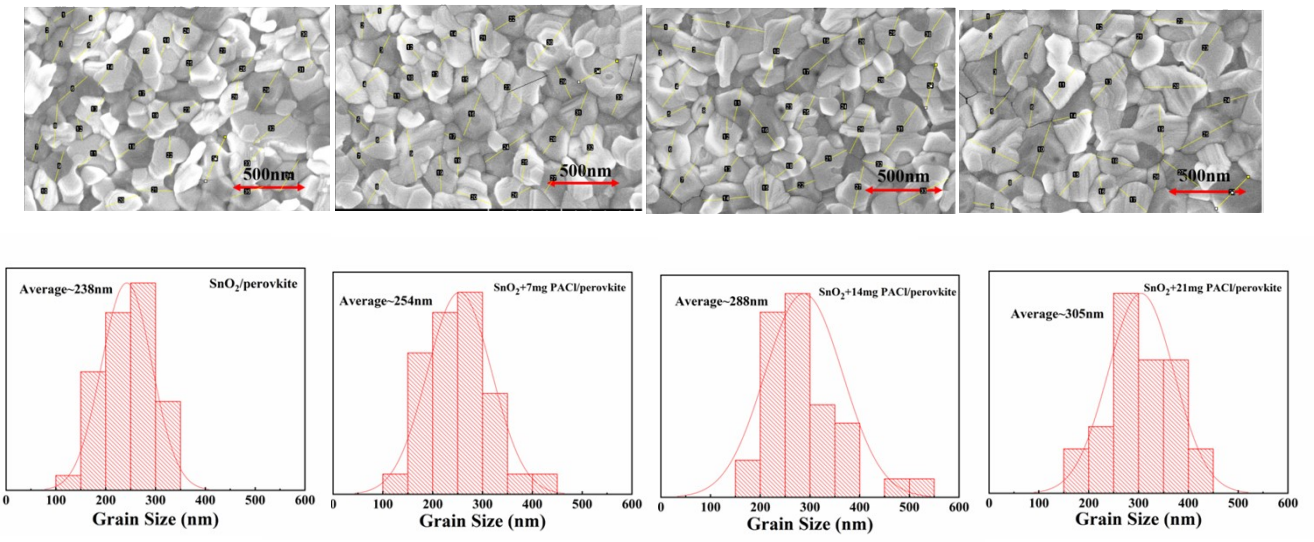


**Figure S7** Grain size distributions of perovskite films based on $SnO_2$, $SnO_2$-7PACl, $SnO_2$-14PACl, $SnO_2$-21PACl films.

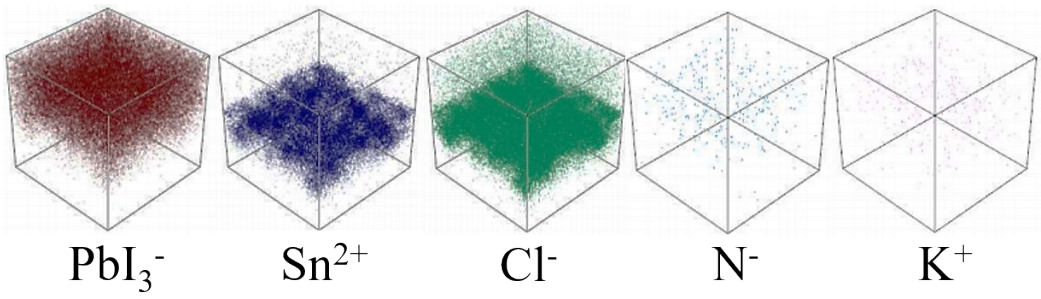


**Figure S8** The 3D depth profiles of ToF-SIMS data.

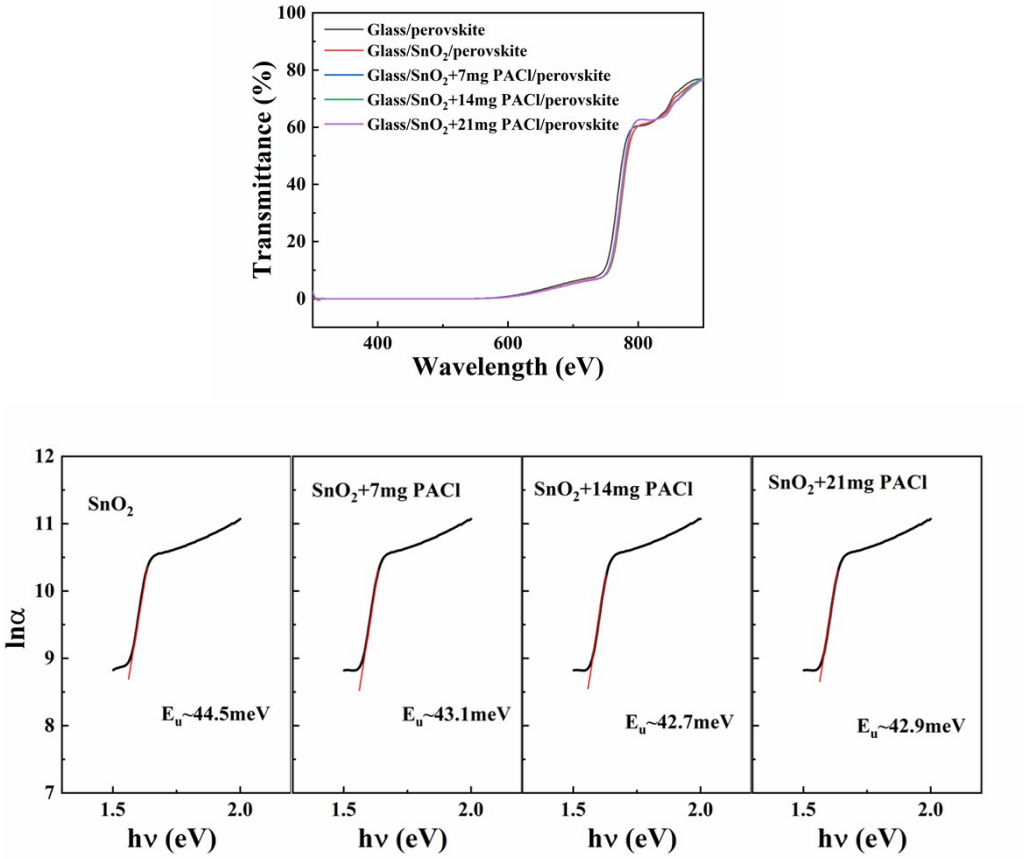


**Figure S9** Transmittance spectra and ln $\alpha$ versus $h\nu$ plots of the perovskite films growth on $SnO_2$, $SnO_2$-7PACl, $SnO_2$-14PACl, and $SnO_2$-21PACl films. According to Urbach law given by $\alpha = \alpha_0 \exp(h\nu/Eu)$, the Urbach energy ($Eu$) is estimated from the slop of ln$\alpha$ versus $h\nu$ plots using the logarithmic form of $\ln\alpha = \ln\alpha_0 + h\nu/Eu$.

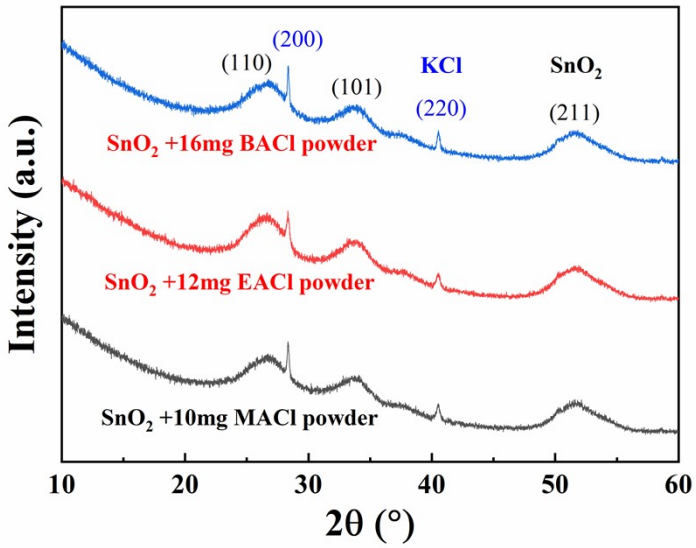


**Figure S10** XRD patterns of the freeze-dried $SnO_2$ powder incorporated with MACl ($CH_3NH_3Cl$, n=1), EACl ($CH_3CH_2NH_3Cl$, n=2) and BACl ($CH_3CH_2CH_2CH_2NH_3Cl$, n=4) in the colloid solution. KCl peaks appear in the XRD patterns of all the samples.

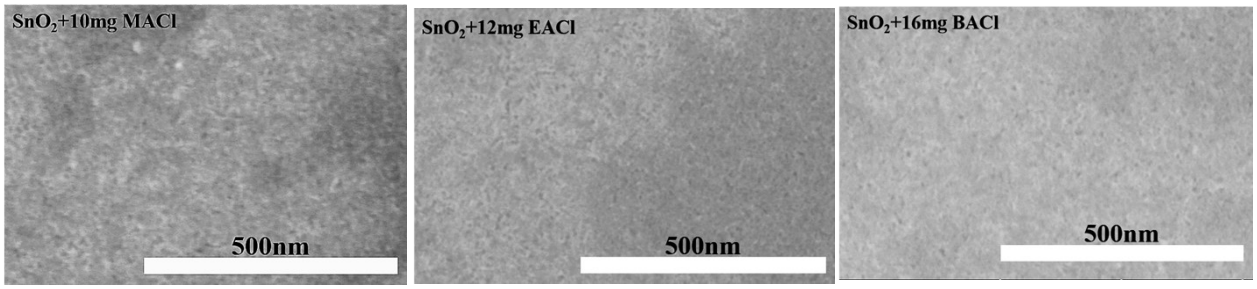


**Figure S11** SEM images of the $SnO_2$ films incorporated with MACl, EACl and BACl. The KCl particles appear on the surfaces of the $SnO_2$ films.

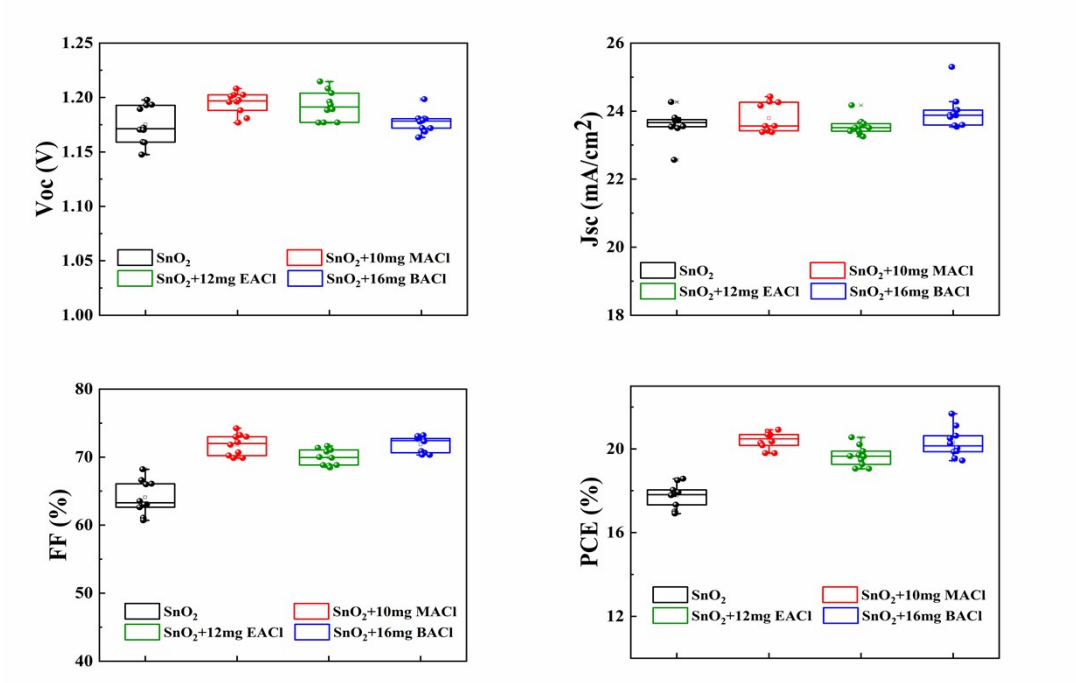


**Figure S12** PV parameters of the PSCs based on $SnO_2$, $SnO_2$-10MACl, $SnO_2$-12EACl, and $SnO_2$-16BACl ETLs, respectively. Improvement of the device performances can be realized on all the PSCs based on primary alkylammonium chloride organic salts incorporated $SnO_2$ ETLs with the most significant improvement in FF, which is consistent with the results of PACl condition.

**TABLE 1** The fitting results of IS.

| ETL | R (Ω cm$^{-2}$) | $R_1$ (Ω cm$^{-2}$) | $R_2$ (Ω cm$^{-2}$) |
|---|---|---|---|
| $SnO_2$ | 6.5 | $2.6\times10^5$ | 8615 |
| $SnO_2$-7PACl | 5.7 | $1.1\times10^4$ | $1.6\times10^5$ |
| $SnO_2$-14PACl | 8.0 | 2689 | $1.83\times10^5$ |
| $SnO_2$-21PACl | 6.3 | 2286 | $1.92\times10^5$ |